

**„CAROL DAVILA” UNIVERSITY OF MEDICINE AND
PHARMACY, BUCHAREST
DOCTORAL SCHOOL
DENTAL MEDICINE**



**CONSIDERATIONS ON METAL ARTIFACTS
IN CONE BEAM COMPUTED TOMOGRAPHY**

PHD THESIS SUMMARY

PhD supervisor:

PROF. UNIV. DR. IONESCU ECATERINA

PhD student:

ROGOJAN (căs. BĂLUȚĂ) ANDREEA MIHAELA

2022

CONTENT

INTRODUCTION	7
CURRENT STATE OF KNOWLEDGE	13
CHAPTER 1. RADIOLOGICAL INVESTIGATION IN DENTISTRY	14
1.1 2D Imaging methods used in dentistry	15
1.1.1. Intraoral radiography	15
1.1.2. Panoramic radiography	17
1.1.3. Cephalometric radiographs	18
1.2. 3D Imaging methods used in dentistry	19
1.2.1. Computed tomography	19
1.2.2. Cone beam computed tomography	21
CHAPTER 2. CONE BEAM COMPUTED TOMOGRAPHY (CBCT)	24
2.1. Obtaining CBCT images	25
2.1.1 Image acquisition	25
2.1.2 Image reconstruction	28
2.2. CBCT unit configuration	32
2.3. Technical parameters of CBCT units	33
2.3.2. CBCT image quality	35
2.3.3. Image projections	37
2.3.4. Rotation arch	38
2.3.5. Field of view (FOV)	38
2.3.6. The image view	38
2.3.7. Image manipulation	39
2.3.8. Monitor display	39
2.3.9. Optical image	40
CHAPTER 3. ARTIFACTS IN CONE BEAM COMPUTED TOMOGRAPHY	41
3.1. Artifacts caused by malfunction and improper adjustment of CBCT unit	41
3.2. Artifacts due to the physical process involved in data acquisition	43
3.2.1. Noise	43
3.2.2. Artifacts due to scattered radiation	44
3.2.3. Artifacts due to beam hardening	44
3.2.4. Extinguishing artifacts	46
3.2.5. Margin Gradient Exponential Artifacts (EEGE)	46
3.2.6. Partial volume artifacts	47

3.3. Patient related artifacts	47
3.3.1. Movement artifacts	47
3.3.2. Metal artefacts	48
CHAPTER 4. METAL ARTIFACTS IN CBCT	50
PERSONAL CONTRIBUTIONS	57
CHAPTER 5. DIRECTIONS, OBJECTIVES AND METHODOLOGY OVERVIEW OF SCIENTIFIC RESEARCH	58
5.1. General objectives. Research directions	58
5.2. General methodology of scientific research	59
5.2.1. CBCT unit	59
5.2.2. Study group	61
5.2.3. Research protocol	65
5.2.4. Processing of research data and statistical tests used	68
CHAPTER 6. STUDY ON THE EFFECTS OF INTENSITY AND TUBE CURRENT VOLTAGE IN CORRELATION WITH POSITION AND TYPE OF METAL IN THE APPEARANCE OF METAL ARTIFACTS IN CBCT SECTIONS	70
6.1. Introduction	70
6.2. Purpose and objectives	71
6.3. Material and method	72
6.4. Results	78
6.5. Discussions	93
6.6. Conclusions	99
CHAPTER 7. STUDY ON THE IMPACT OF METAL ARTIFACTS ON IMAGE QUALITY IN CBCT SECTIONS DEPENDING ON ANATOMICAL POSITION	100
7.1. Introduction	100
7.2. Purpose and objectives	102
7.3. Material and method	102
7.4. Results	108
7.5. Discussions	127
7.6. Conclusions	132
GENERAL CONCLUSIONS	134
REFERENCES	139
ANNEXES	154

INTRODUCTION

The anatomical complexity of the dento-maxillary region determined the need to move from two-dimensional (2D) to three-dimensional (3D) imaging, thus developing volumetric computed tomography, also called cone beam computed tomography (Suomalainen *et al.*, 2007). In CBCT technology, due to the discrepancy between the mathematical model and the physical image processing, artifacts are commonly induced (Schulze *et al.*, 2011). Because they interfere with the process of diagnosis, treatment planning, or monitoring, each physician should recognize their presence. In this regard, it is necessary to evaluate methods that can reduce the occurrence of these artifacts in order to obtain reliable diagnostic information, which would help to develop personalized protocols for exposure and examination of patients, based on information related to their dental medical history, maintaining ALARA principle (As Low As Reasonable Achievable) (Council Directive 96/29 / Euratom, 1996).

The present paper aims to evaluate the metal artifacts based on variables represented by the technical parameters of exposure, the type and position of the metal object, being an analytical study, which verifies the appearance of metal artifacts related to the aforementioned variables. As a large part of the population has prosthetic restorations made of different alloys and implants, it is important to quantitatively assess the effect of the presence of metals in relation to the pattern and intensity of the artifacts produced and, finally, the diagnostic yield of CBCT. The role of this investigation is to help characterize image quality degradation by enhancing X-ray beam and induced scattering on adjacent and regional structures when metallic objects are present in CBCT images, and to identify the appropriate protocol for assessing a particular region in the metal structures vicinity.

The scientific research of my doctoral thesis presents retrospective and experimental observational analytical studies on the optimization of the diagnosis and the need to adapt the guidelines for the use of CBCT investigations depending on the clinical situation encountered. Regarding the subject of the studies, they reach a little explored field due to its niche position, namely the investigation of metal artifacts in CBCT imaging. For this reason, efforts to optimize exposure factors are essential for improving image quality.

The doctoral thesis is structured in 7 chapters, with a general part consisting of the introduction and 4 chapters, followed by the part of personal contribution organized in 3 chapters, to which is added the chapter of general conclusions. Thus, the general part reviews the scientific information on radiological investigation in dentistry, CBCT technology as operating principles and technical considerations, as well as a review of information related to CBCT artifacts in general, with interest in metal artifacts. The personal part, the second section of the thesis, begins with the chapter dedicated to the general methodology of scientific research. Then, my personal studies follow, in accordance with the proposed research directions, to which are added the general conclusions of the paper, as well as the open perspectives aimed at optimizing the diagnosis through CBCT.

- CURRENT STATE OF KNOWLEDGE -

CHAPTER 1. RADIOLOGICAL INVESTIGATION IN DENTISTRY

Similar to other medical fields, radiological investigation in dentistry has proven useful in the diagnosis and treatment of diseases of the oral cavity. Radiology is the first branch of medical imaging, and depending on the field approached, it can include both diagnostic and therapeutic aspects. This chapter outlines the imaging techniques used in dentistry.

CHAPTER 2. CONE BEAM COMPUTED TOMOGRAPHY (CBCT)

Cone Beam Computed Tomography (CBCT) is a general term for a technology that encompasses a variety of devices that differ in many ways: patient positioning, scanned volume size (FOV), radiation characteristics, image capture and reconstruction, image resolution, and radiation dose.

Due to the widespread use of CBCT in dental and maxillofacial imaging, it is important for the user to understand the concepts underlying the operation of this technique and the inherent limitations, especially of artifacts (Pauwels *et al.*, 2015). To maximize patient benefit and minimize the risk of radiation, the complexity of modern CBCT equipment requires a perspective on the various trade-offs involved, and it is essential to understand the various technological factors and scanning parameters that influence image quality and radiation dose. This chapter briefly covers the technical aspects of the CBCT imaging chain, starting from an overview of the principles of CBCT imaging, the configuration and technical parameters of CBCT units.

CHAPTER 3. ARTIFACTS IN CONE BEAM COMPUTED TOMOGRAPHY

In computed tomography, the term artifact is used for any systematic discrepancy between the CT numbers in the reconstructed image and the actual attenuation coefficients of the object. Tomographic images are inherently more exposed to artifacts than conventional radiographs because the image is reconstructed from millions of independent detector measurements (Barrett and Keat, 2004). These artifacts contribute to image degradation and can lead to inaccurate or false diagnoses.

There are several possible causes for artifacts to appear in an image, and it is important for the user to recognize them so that they can be removed or minimized. Depending on the causes, the artifacts may be caused by malfunction and improper adjustment of the CBCT, may be due to the physical process involved in acquiring the data or in connection with the patient.

CHAPTER 4. METAL ARTIFACTS IN CBCT

Metal artifacts are problematic, especially in the dentoalveolar area, due to the frequent presence of metal objects such as metal restorative materials, root-canal posts, crowns, brackets and implants. The metals in the structures present in the field of view attenuate very much the X-ray beam, the value of the attenuation obtained behind the object being incorrectly recorded. When reconstructing the image, a significant degradation of its quality is observed. In CBCT, metal artifacts meet in all directions due to the cone beam (de Man, 2004; Kyriakou *et al.*, 2009). Various effects contribute to the appearance of metal artifacts, such as beam hardening, scattered radiation, quantum noise, photons extinction, and how they appear in the image depends on the severity of these effects on the one hand and the way in which the reconstruction algorithm treats them (de Man, 1999; de Man, 2000; Schulze *et al.*, 2011).

Numerous authors have reported influencing the quality of the CT or CBCT diagnostic image of the head and neck by the presence of metal objects located in the dental area (Holberg *et al.*, 2005; Draenert *et al.*, 2007; Schulze *et al.*, 2010; Perrella *et al.*, 2010; Razavi *et al.*, 2010), other authors investigated the reduction of these metal artifacts using adapted scanning techniques (Haramati *et al.*, 1994; Nakae *et al.*, 2008) or specific reconstruction algorithms or post-processing techniques (Kyriakou *et al.*, 2009; Prell *et al.*, 2009; Wang *et al.*, 2013).

. - PERSONAL CONTRIBUTIONS -

CHAPTER 5. DIRECTIONS, OBJECTIVES AND METHODOLOGY OVERVIEW OF SCIENTIFIC RESEARCH

Due to its advantages, CBCT has become essential in dentistry. Although CBCT images have many advantages, there are some limitations, the most common problem being the formation of artifacts. As I mentioned in the first part of the thesis, the artifacts have different origins. When the artifacts are caused by the patient, they are most frequently and intensely determined by the presence of metallic materials in the examined area (Schulze *et al.*, 2011). Artifacts also appear in connection with X-ray exposure parameters, such as milliamperage (mA) and voltage (kVp) used in image acquisition, which cause more radiation to dissipate in the presence of high-density elements, generating significant changes that compromise image quality and, consequently, diagnosis (Scarfe *et al.*, 2008; Loubele *et al.*, 2009).

5.1. General objectives. Research directions

My *general aim* is to optimize diagnosis in CBCT examination by quantitatively assessing the effect of metal presence correlated with the pattern and intensity of artifacts produced, by developing a configuration representing increasing effects of local and general

artifacts to simulate different clinical scenarios. The specific objectives are detailed in the analytical studies conducted, experimental and observational retrospective.

The study on metal artifacts in CBCT technology was focused on 3 *directions of research*, following the influence of the following factors in the emergence of metal artifacts:

- type of metal
- position of the metal
- CBCT scanner exposure parameters.

In the first study of my research, experimentally, I aimed to quantitatively investigate the effect of the presence of metals in correlation with the effect of independent variables on the quality of CBCT images, the dependent variable. To this end, I investigated the influence of the type of metal inserted, its position at the jaws, as well as the exposure parameters of the CBCT unit: kV (responsible for X-ray beam quality) and mA (which influences the amount of X-rays), which were evaluated in order to validate protocols corresponding to different diagnostic tasks. Thus, regarding the type of metal, I evaluated the most frequently used metals in practice, namely chromium-cobalt alloy, used in crowns and root-canal posts and titanium, used in implantology, quantifying their effects on CBCT image quality.

The second study, retrospective observational, quantitatively evaluates the effect of the presence of metals, represented by titanium implants, and the intensity of artifacts produced depending on the anatomical region where they are inserted (maxillary or mandibular, frontal or lateral), placed isolated or adjacent to each other, as well as their position in the field of view (central or eccentric).

5.2. General methodology of scientific research

5.2.1. CBCT unit

The CBCT unit type and different exposure protocols may change the appearance of the artifacts. In this doctoral research, I used a single CBCT device, type Morita Veraviewepocs 3D (J. Morita, Kyoto, Japan), to improve the comprehensibility and practicability of the study. The model of the unit allows to choose between several types of visual fields, from Ø 40 x 40 mm to Ø 80 x 80 mm, the exposure parameters can be changed manually, for the voltage can opt for the range 60-80 kV, and for the intensity 1 -10 mA. In my doctoral research, I used a visual field of Ø 40 x 40 mm and a partial rotation of 180° for all the exposures. In the first study, I initially used scout images before 3D scanning to ensure the correct placement of the simulated model of the mandibular dental arch, then I used manual exposure protocol, changing the voltage and current parameters within the limits allowed by the equipment manufacturer. In the second study I applied automatic exposure control, obtaining scout images used as a reference for subsequent 3D exposures, using the manufacturer's recommended protocol for an average adult patient, 80 kV and 5 mA.

5.2.2. Study group

The first study was performed on a model that simulates the mandibular arch, made of polyurethane. To simulate the attenuation of radiation in soft tissues, the polyurethane

model was covered with wax about 15 mm thick. The metal structures evaluated in the first study were rods made of titanium, in order to quantify implant-induced artifacts, and chromium-cobalt alloy, a metal often used for root-canal posts. All rods were 2.8 mm in diameter and 15 mm high. The different shapes and sizes of the rods could change the artifacts in CBCT images, and to avoid the impact of irregular morphology and size on the results, in this study I used uniform conical structures, similar in shape to implants or root-canal posts. The titanium rods were made of Titanium Ti6Al4V (manufacturer NTI-Kahla GmbH, Germany), and for maximum accuracy and similarity in size, the chromium-cobalt alloy rods were made by CAD-CAM technology, with ProX DMP 100 type system (3D Systems Inc., South Carolina, USA), the metal used for laser sintering being an alloy of chromium (24.7%) - cobalt (63.9%) free of nickel and beryllium (Mediloy S-CO, BEGO Bremer Goldschlägerei Wilh Herbst GmbH & Co. Bremen, Germany).

Subsequently, at the level of the model, 3 parallel holes were made by milling, with dimensions corresponding to the manufactured rods, in the canine area, the second premolar area and the distal root of the 6-year-old molar, at equal distances from each other. To make the preparations we used the drills provided by the manufacturer of titanium rods. The model thus made was fixed on the platform of the CBCT unit, on the basis provided by the manufacturer, placed in the center of the FOV and aligned with the horizontal plane using the laser light system for orientation. The model was scanned several times applying different exposure parameters, initially the control model, without rods, and subsequent exposures were used on the test model, with the removal and replacement of titanium rods and chromium-cobalt alloy successively, without change the position of the model on the platform of the CBCT unit. The scanning protocols used were different, either by varying the current in tube (1mA, 5mA, 10mA) or the voltage (60kV, 70kV, 80kV). The total number of scans performed was 27, equal to the number of exposure settings used, 9, multiplied by the configurations used, 3.

In the second study, the CBCT sections with implants used were selected from the archive of a private practice practice in Bucharest. Patients provided informed consent and agreement to participate in medical education to the prescribing doctor of the radiological investigation, and the retrospective study was in accordance with the 1975 Helsinki Declaration, revised in 2000, with the consent of the unit. In the research sample I included CBCT examinations that presented quality images of implants, of patients of both sexes and of any age, made in a period of 2 years. Acquisitions with movement artefacts, with implants without the presence of prosthetic crown and in the vicinity of teeth with large fillings with increased radiopacity, metal crowns or root-canal posts and FOV different from $\text{\O} 40 \times 40$ mm were excluded. Depending on the position in the FOV, the implants were classified as having a central or eccentric position, and depending on the proximity of other implants, they were divided into isolated or adjacent. For each selected case, 3 axial reconstructions were chosen, one in the cervical third, one in the middle third and the third in the apical third, perpendicular to the center of the implant.

5.2.3. Research protocol

After obtaining scans and multiplanar reconstructions, the volumetric data was reconstructed using the i-Dixel software, version 6.4.0.6. In a first stage, images in the axial section were selected, the regions of interest were chosen, and then the quantification of the

metal artifacts was performed. Selected appropriate axial section images were exported for quality assessment as DICOM files from i-Dixel software and imported into Image J software (NIH Image National Institutes of Health, Bethesda, MD, USA) for analysis, saved as "png." image, in a two-dimensional shape used for comparison.

Selection of images and regions of interest (ROI)

In the first study, the images were viewed by two observers with experience in CBCT imaging. All reconstructions evaluated by the observers were selected at the same axial level, with the automatic setting of the window / level in most cases, the manual adjustment being performed if the automatic setting was considered to be below the optimal parameters. The axial plane perpendicular to the rod located in the premolar area, 3 mm below the surface of the polyurethane model, was selected as the reference plane. Observers selected eight 10 x 10 pixel rectangular areas of interest (ROI). These regions included the regions adjacent to the vestibular surface and the lingual surface of the rods, and the median regions corresponding to an imaginary line connecting the anterior rod to the middle and the middle rod respectively to the posterior one (fig. 5.7.).

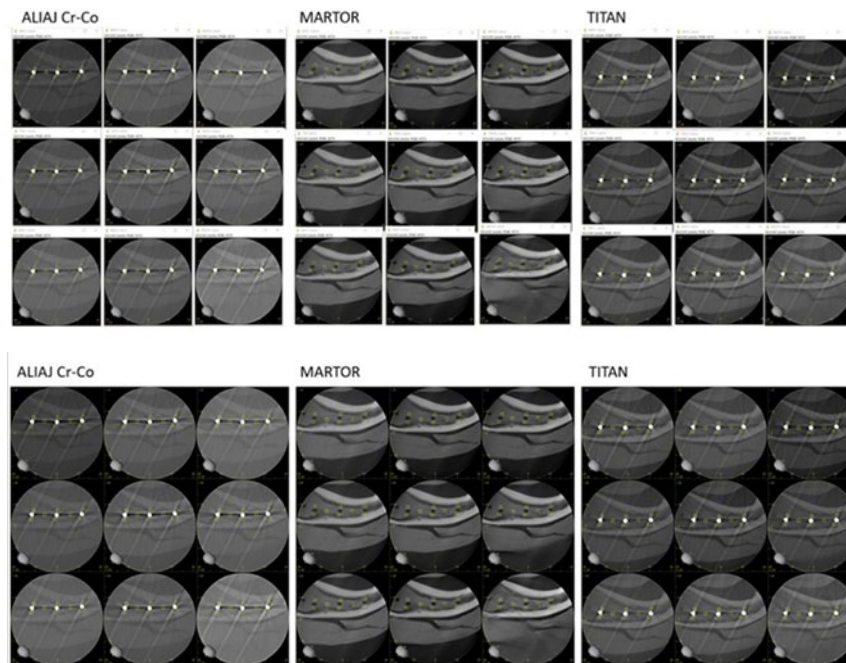


Figure 5.7. Axial two-dimensional images and regions of interest used to measure gray values in the first study (top-first evaluator; bottom-second evaluator)

For the second study, only one examiner, experienced in CBCT imaging, was responsible for choosing the images as well as the axial sections of each selected implant, with 30% of the exams being re-evaluated after two weeks. The same monitor was used as in the previous study. For each implant, three axial reconstructions were chosen, one in the cervical third, which allowed the entire diameter of the implant to be visualized before the prosthetic connection, one in the apical thickness, which allowed the entire diameter of the implant to be visualized in the apical area, and one in the middle third. located halfway between the 2 (Figure 5.8.).

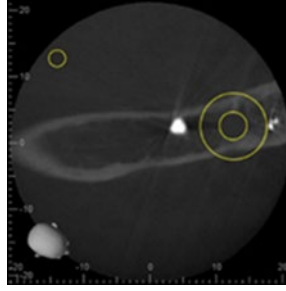


Figure 5.8. Axial section of an implant with ROI positioning defined in ImageJ.

Quantification of artifacts

In order to eliminate the subjective differences between observers, as different observers or even the same observer, at different times, may offer different evaluations for the same image, in my research I adopted methods of quantitative evaluation of metal artifacts, which are detailed in Chapters 6 and 7 of my thesis.

In the first study, using the ImageJ software, the regions of interest for all images were standardized, both for the control model and for the test models. The same protocol was used for all images with test and control models. Subsequently, the average gray level (GV) of the regions of interest was determined. The average GV measured within the ROI defined on the control model for each scan parameter was designated as GV_{control}. Image quality was measured as a percentage difference between the gray values ($\Delta GV\%$) on the control model and the test models, by the method of Benic *et al.* (2013) adapted to this research:

$$\Delta GV\% = \frac{GV_{\text{test}} - GV_{\text{control}}}{GV_{\text{control}}} * 100$$

The quantification of metal artifacts in the second study was done with the same software, ImageJ. In this study, two areas of interest (ROI) were selected for each image with CBCT sections and the gray values and standard deviations were measured. The first region of interest was chosen in the axial view of the implant and encircled the entire implant circumferentially except for the metal itself. The size of this region of interest has been standardized to 10 mm in diameter. I have excluded metal from ROI because in some cases the voxel values were saturated far outside the metal area, and in other cases unsaturated voxel values were found in the center of the metal, similar to the study by Pauwels (2013). Removing the metal from the selection was done manually, as no standardized segmentation method was available using an ImageJ function. The second region of interest, the control area, was selected at the edge of the volume in which the artifact is minimal, according to the recommendations of the protocol of the International Atomic Energy Agency (2017). Standard deviation (SD) and contrast-to-noise ratio (CNR) of titanium implant images were analyzed using the following formula:

$$CNR = \frac{|Mean_{\text{Im plant}} - Mean_{\text{Control}}|}{\sqrt{SD_{\text{Im plant}}^2 + SD_{\text{Control}}^2}}$$

5.2.4. Processing of research data and statistical tests used

The collected data were statistically processed using Microsoft Office Excel 2013. Prior to the analysis, the grouped independent variables were analyzed to determine normality, using the Kolmogorov-Smirnov test, and equal variations, using the F test for normally distributed data, and Levene test for abnormally distributed data. In order to detect the relevance, the 95% confidence interval (CI) was calculated for the values obtained, the level of statistical significance (p) being set at a maximum of 0.05.

In the case of the first study, a correlation coefficient (absolute correlation type) was made for the evaluation of the inter-observer agreement, and this was 99.9%. The values used to quantify the artifacts were represented by the average measurements of the two evaluators. To evaluate the effects of the 4 factors (voltage, current, metal type, position of objects) in the appearance of metal artifacts, the interactions between the variables were calculated. For the comparison of other factors, with more than two categories, the “one-way ANOVA” tests were used, then the post-hoc tests “Tukey’s HSD” or “Gawes-Hawell” for the comparison of pairs. The significant level was considered to be <0.05. The data obtained are presented in the tables in Chapter 6.

In the second study, the measurements were performed by the same examiner who selected the CT sections, with 30% of the examinations being re-evaluated after two weeks to calculate the intraobserver agreement, which was 99.9%. The standard deviation and the contrast-to-noise ratio of the images with titanium implants were analyzed, for the normally distributed data a variance analysis (ANOVA) and the Mann-Whitney test were performed, and for comparing the data corresponding to the cervical, middle and apical images the Kruskal - Wallis and the Tukey test.

The data collected and statistically processed of the studies were subsequently reported to other specialized studies, allowing the conclusions of my scientific research to be established.

CHAPTER 6. STUDY ON THE EFFECTS OF INTENSITY AND TUBE CURRENT VOLTAGE IN CORRELATION WITH POSITION AND TYPE OF METAL IN THE APPEARANCE OF METAL ARTIFACTS IN CBCT SECTIONS

6.1. Introduction

The presence of artifacts is common in current CBCT practice, as they are induced by the discrepancy between the mathematical model and the physical image processing. An artifact of the tomographic image is defined as a visualization of a structure from the reconstructed data that is not present at the level of the subject to be investigated. According to Schulze (2010), the magnitude of artifacts is dependent on the composition of the scanned object, by the number and atomic density of the constituent material, which changes the X-ray spectrum, acting as a filter. Exposure parameters also play a role in the production of artifacts. As an objective in the use of CBCT is the accurate measurement and observation of anatomical structural details, the evaluation of methods that can reduce metal artifacts is

of significant value. In 2011, Schulze stated that there is no standard parameter useful in quantifying the magnitude of artifacts, given the wide variety of scanning devices and protocols available. Among the factors considered effective in improving the image quality are exposure parameters, which are adjustable in some CBCT units.

6.2. Purpose and objectives

The *aim* of this study was to experimentally evaluate the effect of metal artifacts on axial imaging obtained by CBCT system technology.

Following a number of variables of interest, the *objectives* of the study were to determine whether:

- there are effects on the quality of CBCT images in the presence of metal structures;
- there are differences in the quality of CBCT images depending on the type of metal evaluated;
- there are differences in the quality of CBCT images in the presence of metal structures in correlation with the acquisition parameters (mA, kV);
- there are differences in the quality of CBCT images in the presence of metal structures depending on their position in the arches;
- there is a general exposure protocol appropriate for the assessment of the entire oral cavity.

6.3. Material and method

The study was performed on a model made of polyurethane, presented in detail in Chapter 5 of this research, using 3 metal rods made of chromium-cobalt and titanium alloy. Titanium rods have been used to evaluate artifacts induced by dental implants, titanium being the most commonly used metal in their manufacture, CBCT assessments are often performed both in the initial phase and in the monitoring stages. Cr-Co rods have been used to evaluate artifacts in the case of root-canal posts, which make it difficult to diagnose endodontic or periodontal disease. The protocol followed by the evaluators in selecting the regions of interest is described in the chapter on general research methodology and in Annex 1.

6.4. Results

Two approaches were used to analyze the data:

- Descriptive statistics to view and describe trends for each metal type, metal object position and exposure parameters used,
- Statistical comparison, analytical, for the effects of classified independent variables.

The working hypothesis was represented by the difference in gray values ($\Delta GV\%$) as an index of image quality. Interpretation of values for $\Delta GV\%$ was as follows:

- the difference in gray values ($\Delta GV\%$) close to zero (0) means that there is only a small or no difference in image quality between the model without inserts (control) and the model with inserts (test),
- the difference in gray values with negative values ($-\Delta GV\%$) describes a relatively hyperdense or dark region, associated with beam hardening,
- the difference in gray values with positive values ($+\Delta GV\%$) corresponds to a relatively hypodense or bright region, associated with the scattered radiation.

This difference in gray values was calculated for each type of metal used, titanium or chromium-cobalt alloy, each position of the rods and for each scan parameter used, milliamperes and kilovolts.

Image quality for titanium

In Figure 6.5. and according to the post-hoc tests on the image quality (Δ GV%) for titanium, the following are noted:

- image quality is generally reduced due to metal effects by increasing the overall image density due to beam hardening ($-\Delta$ GV%),
- beam hardening effects are predominant (in 64 of 72 positions),
- the effects on the gray values appear independently of the position of the rod,
- the effects caused by the beam hardening are generated independently of kV and mA,
- HSD tests showed statistically significant differences between protocols ($P = 0.00013$), in 8 comparisons, 60kV / 5mA protocols with 60kV / 10mA, 60kV / 10mA and 80kV regardless of mA,
- image quality was better for all protocols that used 80kV, 80kV / 10mA and 70kV / 5mA and 70kV / 10mA protocol,
- post-hoc tests had statistically significant differences ($P < 0.0001$) when assessing the positions tested in half of the cases,
- the greatest deterioration of the image quality appears in the positions of the middle regions corresponding to the imaginary line that connects the anterior rod to the middle one, respectively the middle one to the posterior one, followed by the lingual area of the canine,
- the increase of kV determined the reduction of the artifacts in the positions adjacent to the lingual and vestibular rods ($P < 0.00014$),
- in all titanium samples, the artifacts between the middle and front rods were more intense than in the region between the rear and middle rods ($P < 0.05$)

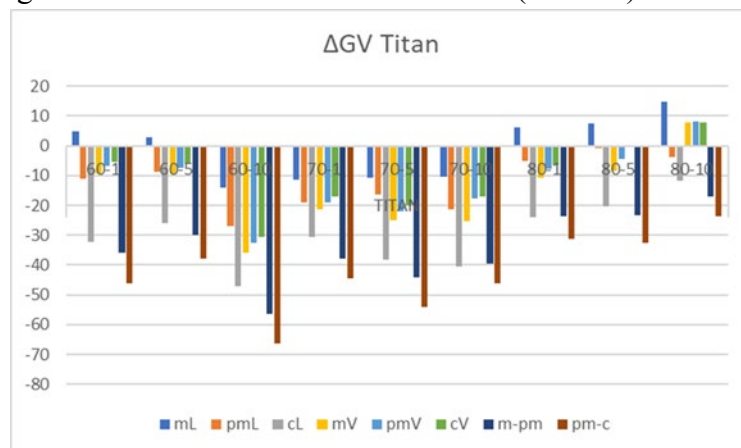


Figure 6.6. Total graph of Δ GV% for titanium.

Image quality for chromium-cobalt alloy

The image quality (Δ GV%) for the chromium-cobalt alloy is highlighted in Figure 6. In the case of this alloy, the following conclusions can be drawn:

- the presence of artifacts is independent of the rod position,

- cobalt-chromium alloy produced significantly more intense artifacts than titanium in all positions ($p < 0.000040$),
- the beam hardening effects are lower compared to titanium ($-\Delta GV\%$) and the scattering effects are higher,
- scattering effects are visible in most vestibular and oral positions of the rods (in 36 out of 54 positions).
- HSD tests showed statistically significant differences between protocols ($P = 0.0002$), between 60kV / 1mA and 60kV / 10mA, 70kV / 10mA, 80kV / 1mA, 80kV / 10mA and 70kV / 1mA with 80kV / 10mA protocols,
- the post-hoc tests had statistically significant differences ($P < 0.0001$) in the evaluation of the tested positions compared to the positions between the rods,
- there were no significant differences compared to the position “between the rear and the middle rod” with the position “between the middle and front rod” in all conditions ($P > 0.05$).
- the values adjacent to the posterior lingual rod and the anterior vestibular rod were significantly higher than those of the other two intermediate positions ($P < 0.00003$).
- the change in voltage did not reduce the artifacts ($P > 0.05$)

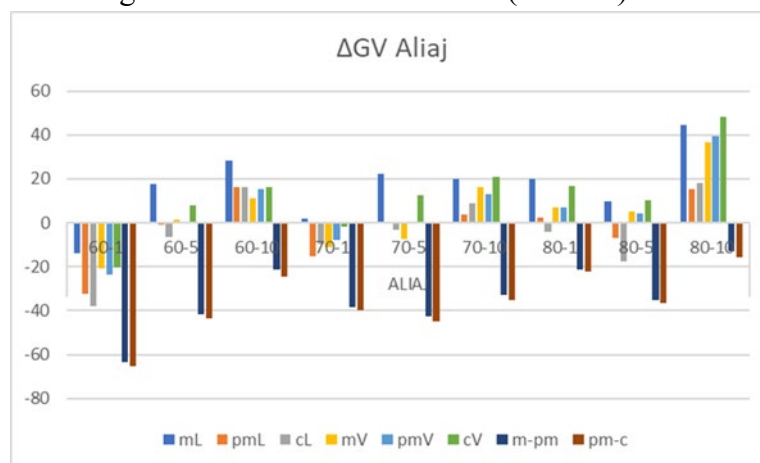


Figure 6.6. Total graph of $\Delta GV\%$ for chromium-cobalt alloy.

Image quality depending on the position of the metal rod

Another variable investigated in relation to image quality ($\Delta GV\%$), was the position of metal structures, for which the following are observed:

- image quality is generally reduced due to metal effects, either by increasing the overall image density due to beam hardening ($-\Delta GV\%$) or by scattering effects ($+\Delta GV\%$), as seen in Figure 6.7.
- beam hardening effects are predominant,
- the effects on the difference in gray values appear regardless of the position of the rod,
- image quality effects are generated independently of kV and mA,
- statistical analysis shows significant difference between positions ($P < 0.0001$),
- the greatest deterioration in image quality occurs in the positions of the middle regions corresponding to the imaginary line connecting the anterior rod to the middle,

followed by the imaginary line connecting the middle rod to the posterior, and the lingual area of the canine, through beam hardening effects ($-\Delta GV\%$), and the change in protocol does not appear to affect the degree of image degradation,

- the slightest damage is noticeable in the lingual areas of the middle rods, for chromium-cobalt alloy, and posterior for titanium.



Figure 6.7. Total graph of $\Delta GV\%$ by position.

Image quality depends on voltage variation

Regarding the image quality ($\Delta GV\%$) depending on the voltage variation, another parameter investigated, from figure 6.8. and post-hoc tests, the following are highlighted:

- image quality is generally reduced due to the effects of inserted metals,
- beam hardening effects are predominant ($-\Delta GV\%$),
- the effects produced are generated independently of the kV variation ($P = 0.0003$),
- post-hoc tests had statistically significant differences ($P < 0.001$, according to the Kruskal-Wallis test) in assessing the influence of stress on the 2 types of metals, with the most statistically significant difference in the Mann-Whitney test ($P < 0.0001$) between 70kV protocols for titanium and 80kV for chromium-cobalt alloy,
- the largest statistical difference between titanium and chromium-cobalt alloy occurs when using the voltage of 70kV ($P < 0.0000003$),
- the increase of kV determined the reduction of the artifacts in the positions adjacent lingual and vestibular to the anterior and posterior stems ($P < 0.024$),
- the increase in kV did not reduce the artifacts in the intermediate positions between the rear and middle rods and between the middle and front rods

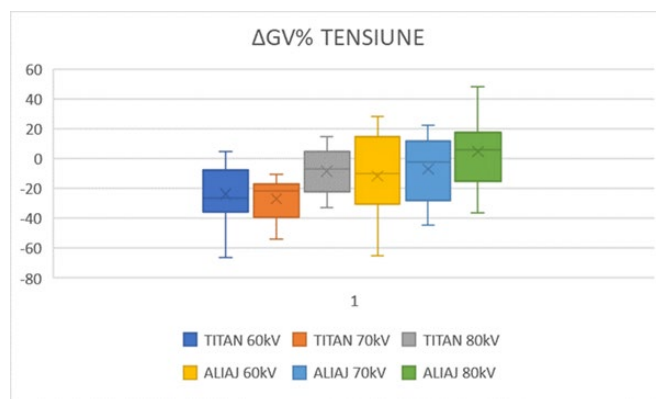


Figure 6.8. Total graph of $\Delta GV\%$ depending on the voltage used.

Image quality depends on intensity variation

Figure 6.9. shows the image quality ($\Delta GV\%$) in relation to the change in current intensity, with the following characteristics:

- image quality changes due to the effects of inserted metals,
- the beam hardening effects are predominant ($-\Delta GV\%$), the scattering effects being characteristic of the 10mA current in the case of the alloy,
- the present effects are generated depending on the mA variation in the case of chromium-cobalt alloy ($P = 0.0003$), beam hardening ($-\Delta GV\%$) for intensities of 1 and 5 mA for both titanium and alloy, and scattering for 10mA alloy,
- the change in the intensity of the tube current did not affect the artifacts ($P > 0.05$), except for the lingual area of the anterior rod ($P = 0.03$),
- post-hoc tests had statistically significant differences ($P < 0.0001$) in assessing the influence of intensity compared to the 2 types of metals.

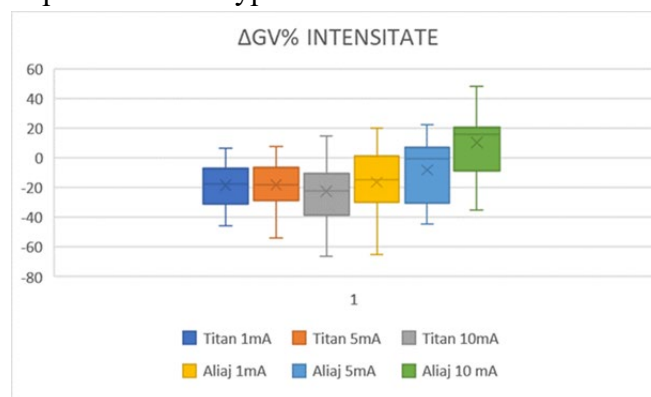


Figure 6.9. Total graph of $\Delta GV\%$ depending on the current intensity used.

Image quality depends on the scan protocol used

The scan protocol used determined the following changes in image quality ($\Delta GV\%$):

- image quality is generally reduced due to the effects of the inserted metal
- beam hardening effects are predominant ($-\Delta GV\%$), as seen in Figure 6.10,
- there is a statistical difference between the scanning protocols tested ($P < 0.0004$),
- the present effects are generated independently of kV and mA,
- post-hoc tests show a statistically significant difference between the 80kV-10mA protocol and the 60kV-1mA, 60kV-10mA, 70kV-1mA and 70kV-5mA protocols, regardless of the type of metal inserted and its position.

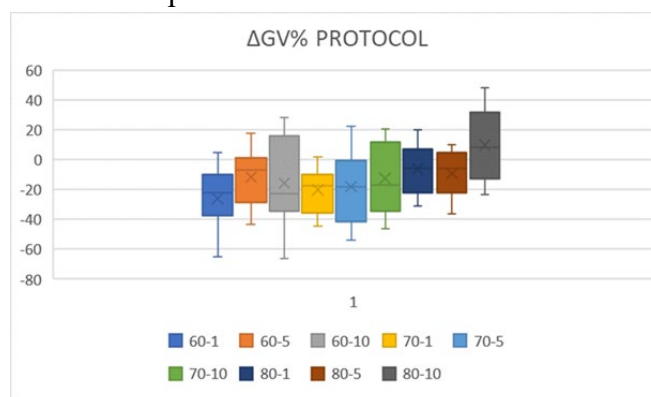


Figure 6.10. The total graph of $\Delta GV\%$ depending on the scanning protocol used, regardless of the type of metal and the position of the rod.

Tables VI.12. and VI.13. identifies the top three Morita Veraview 3De scanner settings for each position and type of metal inserted.

Table VI.12. The best 3 combinations of device settings for each position evaluated in the case of titanium rods

Poziția		Protocol		
		1	2	3
molar	lingual	60kV-5mA	60kV-1mA	80kV-1mA
	vestibular	80kV-10mA	80kV-5mA	60kV-5mA
premolar	lingual	80kV-5mA	80kV-10mA	80kV-1mA
	vestibular	80kV-5mA	60kV-1mA	60kV-5mA
canin	lingual	80kV-10mA	80kV-5mA	80kV-1mA
	vestibular	80kV-5mA	60kV-1mA	80kV-1mA
zona molar-premolar		80kV-10mA	80kV-5mA	80kV-1mA
zona canin-premolar		80kV-10mA	80kV-1mA	80kV-5mA

Table VI.13. The best 3 combinations of device settings for each position evaluated for chrome-cobalt alloy rods

Poziția		Protocol		
		1	2	3
molar	lingual	70kV-1mA	80kV-5mA	60kV-1mA
	vestibular	60kV-5mA	80kV-5mA	80kV-1mA
premolar	lingual	70kV-5mA	60kV-5mA	80kV-1mA
	vestibular	60kV-5mA	70kV-5mA	80kV-5mA
canin	lingual	70kV-5mA	80kV-1mA	60kV-5mA
	vestibular	70kV-1mA	60kV-5mA	60kV-10mA
zona molar-premolar		80kV-10mA	60kV-10mA	80kV-1mA
zona canin-premolar		80kV-10mA	80kV-1mA	60kV-10mA

ANOVA and post-hoc tests indicated that the alloy rods produced more artifacts than the titanium rods, according to the standard deviation values ($p < 0.00004$). The change in tube current intensity did not affect the artifacts ($P > 0.05$), except for the lingual area of the anterior rod ($P = 0.03$). The increase in kVp, in general, led to a reduction in metal artifacts ($P = 0.04$) in positions adjacent to the front and rear rods in particular, not having a significant impact on the intermediate positions between the rear and middle rods and between the middle and front rods.

6.5. Discussions

The measured values for all positions and protocols are a general estimate of the influence of the metal on the voxel values in that region, and the larger deviations correspond to the larger artifacts. In general, when a polychromatic X-ray beam passes through an object, low-energy photons are absorbed more than high-energy photons. This phenomenon increases the average energy of the X-ray beam, causes the beam to harden and disrupts the image reconstruction process. A lower energy of the X-ray beam, a higher density and an irradiated substance with a higher atomic number lead to a higher hardening of the beam, the artifacts being thus more severe when the metal is present (Schulze *et al.*, 2011; Pauwels *et al.*, 2015). According to the results of this experimental study, extinguishing artifacts and lower gray values are observed between the two metal rods

anterior and middle, respectively medium and posterior. This is due to the fact that when the X-ray beam passes through two metal rods simultaneously, the beam hardening is more severe (White and Pharoah, 2014; Kuusisto *et al.*, 2015). In this study, the metal artifacts adjacent to the anterior vestibular and posterior lingual rods were more intense than those of the other positions, which may be due to different projection paths, information processing, and reconstruction techniques. There may be different results when using different CBCT units, as seen in studies by Schulze *et al.*, (2010) or Benic *et al.*, (2013) where the implant site did not affect the severity of the artifact.

Comparisons between titanium and cobalt-chromium alloy revealed that in all eight positions and when using any combination of exposure parameters, the artifacts induced by cobalt-chromium rods were more intense than those observed in titanium exposures. Cobalt-chromium-induced low-value artifacts were more severe than titanium in the region between the middle and front rods, but both this position and that between the rear and middle rods generated the most intense artifacts in both conditions. Thus, the gray value between the two cobalt-chromium or titanium inserts with different exposure parameters underwent the largest changes. The gray values of these regions were therefore severely underestimated. The CBCT imaging system uses an X-ray beam with polychromatic energies which, by selectively attenuating lower energy photons as the beam passes through high density structures, causes the beam to harden, in direct connection with the cube of the atomic number (Z) of the structure traversed by X-rays, so the higher the atomic number, the higher the amplitude of the beam-hardening effect. Because the atomic numbers of chromium ($Z = 24$) and cobalt ($Z = 27$) are higher than that of titanium ($Z = 22$), and cobalt-chromium alloys are used in dentistry in the composition of which there are other metals with a higher atomic number, for example molybdenum and tungsten, X-ray absorption and beam hardening were higher in the case of cobalt-chromium alloy than in that of titanium. Studies by Pauwels *et al.* (2013) and Kuusisto *et al.* (2015) reported severe artifacts in CBCT images produced by lead and stainless steel, respectively zirconium and titanium. The study by Chindasombatjareon *et al.* (2011), evaluated the artifacts produced by four metals and found that the investigated gold alloy, with $Z = 79$, caused the largest areas of artifacts followed in order by the cobalt alloy ($Z = 27$), chromium ($Z = 24$), titanium ($Z = 22$) and aluminum ($Z = 13$), supporting the idea of hardening the X-ray beam with increasing atomic number.

From the perspective of the kV variable, its increase generally led to a reduction of metal artifacts in positions adjacent to the anterior and posterior rods, but did not affect the severity of the artifact in the positions between the rods. Previous research (Barrett and Keat, 2004; Schulze *et al.*, 2010; Kataoka *et al.*, 2010; Chindasombatjareon *et al.*, 2011) found that higher voltage and higher penetration are generated as voltage of the X-ray beam increases, so there is less beam hardening and fewer metal artifacts. Also, high kVp reduces contrast, which can contribute to greater image homogeneity. The device used in this study allowed the selection of voltage in the range of 60-80 kVp. This range is not the typical voltage range of CBCT devices, most of which are between 80 and 120 kVp. As a result, it was not possible to study the absolute effect of kVp in a relevant range. Other factors that could affect beam hardening include the rotating arc of the machine, the configuration of the X-ray beam, and the algorithms used for information processing, which are not evaluated in this research (Schulze *et al.*, 2005; Hunter *et al.*, 2009).

Another variable investigated was the intensity of the tube current. Similar to the study by Pauwels (2013), the increase in current intensity did not affect the presence of metal artifacts in most cases in this research, except for the lingual area of the anterior rod, where a reversal of $\Delta GV\%$ occurred. In Pauwels's (2013) study, mAs appear to have varied between protocols due to differences in the number of projections acquired, as exposure time, using more types of CBCT scanners, rather than due to anodic current, which did not happen in this study, where the number of projections was the same. Although theoretically a higher number of projections should lead to reduced artifacts, in Pauwels' study there was no noticeable difference between high mA and low mA protocols for some devices, and the increase in dose following the increase in mA did not. would be justified. In Kataoka's (2010) study, using CT, the higher currents of the tubes decreased the metal artifacts, but we must take into account the intensity range used in that study (100-500mA), which was different from that used in the present study (1-10mA). Because CBCT has a limited range of changes in the mA value, the insignificant effect of the mA change on metal artifacts can be explained.

According to my study, there is no general exposure protocol suitable for assessing the entire oral cavity, but there are configurations of setting exposure parameters in accordance with different diagnostic tasks. However, in order to help make professional decisions about the protocol of choice for specific clinical indications, the correlation with the ALARA principle should be made (as low as reasonable possible). In this study, I identified the best three settings for the scanner exposure parameters used for each position and type of metal inserted, but which may be different when using other CBCT units, as reported by other research, Parsa *et al.* (2010), Bechara *et al.*, (2012) or Fontenele *et al.*, (2018). Some of the best combinations of exposure parameter settings were the same for titanium and chrome-cobalt alloy rods. In addition, these combinations are clearly distinct from each other in terms of variation in gray values, with different protocols acting differently for each type of metal, and the decision to choose a particular setting is necessary to take into account the type of material present in the scan region.

A limitation of this in vitro study was related to the fact that the model used had uniform densities, while the trabecular bone density is not uniform. Of course, the model used does not contain the distinctive features found in the dentomaxillofacial region, but this is not necessarily to analyze the technical performance of image quality, given that the values and noise of the voxel are primarily affected by the total mass inside and outside FOV and not the shape or attenuation range of the scanned object.

The results of my study are difficult to interpret in terms of image quality because there is no frame of reference for parameters associated with metal artifacts. Previous research has shown that there is a wide range of opinions regarding the perceived or measured image quality for CBCT devices in dentistry (Suomalainen *et al.*, 2007; Loubele *et al.*, 2009). Furthermore, large-scale diagnostic imaging studies are not available to assess the relationship between measurable technical parameters in quality control and diagnostic validity, and there are no specific guidelines for clinical imaging performance requirements. for CBCT devices used in dentistry. Hence the need for clear diagnostic criteria to ensure that the technical parameters of the image can be interpreted in a relevant way. Obtaining a

detailed image quality protocol, which would contain thresholds for reviewing or suspending these parameters, thus becomes indispensable.

6.6. Conclusions

The results of the experiments indicated the type of metal as having the greatest effect on the intensity of the metal artifacts in this study, the artifacts induced by cobalt-chromium alloy being more severe than those induced by titanium, and those scans being more affected by different protocols than titanium. The artifacts were more intense on the vestibular surface of the anterior titanium rods and on the lingual surface of the rear alloy rod. The increase in tube current had no effect on the metal artifacts. All this highlights how the protocols work differently for each metal object inserted in the oral cavity, as well as how the choice of acquisition protocol can influence the image quality, especially for structures made of high atomic number metals, taking into account the type of material present in the scan region, the image quality required for diagnosis, and the radiation dose to the patient.

CHAPTER 7. STUDY ON THE IMPACT OF METAL ARTIFACTS ON IMAGE QUALITY IN CBCT SECTIONS DEPENDING ON ANATOMICAL POSITION

7.1. Introduction

The success of implant treatment in dentistry depends mainly on the long-term sustainable health of the peri-implant tissue. Assessment of mobility, pain, infection, inflammation, and marginal alveolar bone loss are all considered useful criteria for successful implantation (Jones and Cochran, 2006). Specifically, attention has been shifted over time to postoperative radiographic evaluation of marginal alveolar bone loss around implants by serial intraoral radiographs (King *et al.*, 2002; Kamburoğlu *et al.*, 2012), with numerous oral radiology guidelines recommending current CBCT as a preoperative examination (Tyndall *et al.*, 2012; SEDENTEXCT Project, 2012). Because it is a three-dimensional examination without overlaps, CBCT has been indicated in dentistry for monitoring implant treatment, in assessing bone regeneration, detecting possible marginal bone loss and signs of failure in osseointegration (Benic *et al.*, 2013). However, CBCT is not part of the routine protocol for postoperative examinations of dental implants due to the limiting factor associated with CT scans, namely the formation of metal artifacts, which may prevent or hinder the proper diagnosis and / or analysis of the periimplant area (Scarfe *et al.*, 2008 Vasconcelos *et al.*, 2017; Machado *et al.*, 2018), compromising image quality.

The research of Oliveira (2013) and Valizadeh (2015) suggests that the formation of metal artifacts may be influenced by the scanned anatomical region, the position of the object in the visual field and adjacent anatomical structures outside the visual field, but there is no consensus on which regions (maxilla or mandible, anterior or posterior area) are more related to the formation of artifacts or what are the effects of the location of the object in the visual field.

7.2. Purpose and objectives

The *aim* of this study was to evaluate, on CBCT images, the metal artifacts produced by titanium implants.

In this sense, the *objectives* of the study were to make a quantitative comparison of:

- artifacts produced in the jaw and mandible;
- artifacts present in the frontal and lateral regions;
- artifacts produced in the vicinity of isolated implants and adjacent to other implants;
- the artifacts displayed depending on the position of the implant within the field of view.

7.3. Material and method

CBCT images of the implants used in this study were selected from the archives of a private practice in Bucharest. The protocol was presented in the chapter dedicated to "General methodology of scientific research". The standard deviation and the contrast-to-noise ratio of the titanium implant images were determined. The standard deviation (SD) was evaluated in order to obtain a general estimate of the magnitude of darkness and brightness/lightness generated by the metal on the values of the surrounding voxels, as a method of measuring noise / artifacts in the image. Among the parameters recommended to be evaluated in the protocol "Quality control in cone beam computed tomography" of the International Atomic Energy Agency (de Las Heras Gala *et al.*, 2017) is the low contrast resolution, which can be quantified by measuring the contrast-to-noise ratio (CNR), considered to be more closely related to image quality than image noise (Grech *et al.*, 2013). CNR is very dependent on local contrast. As the CNR is increased, the objects are more easily visualized in relation to the background, and the reduction of the CNR decreases the detectability of the objects (Bechara *et al.*, 2012a; Bechara *et al.*, 2012b; Bechara *et al.*, 2012c; de Las Heras Gala *et al.*, 2017).

7.4. Results

A total of 80 titanium implants were evaluated, divided into groups according to their anatomical location, proximity to other implants and position within FOV.

Data analysis was performed using two approaches:

- descriptive, to visualize and describe the trends for each axial section of the arches, the position of the implant at the level of the arch, the proximity to other implants and the position within the field of view,
- analytically, for the effects of independent variables.

Descriptive statistics - The cervical section

The descriptive analysis of the cervical axial sections shows the following:

- the highest SD values are representative of the maxillary frontal group, indicating higher artifact production,
- higher SD values for maxillary sections than mandibular ones
- higher SD values for front sections than lateral sections.
- CNR values were lower for the lateral mandibular area in general, so a lower image quality,
- lower CNR values in the mandibular sections than in the maxillary ones
- lower CNR values in the lateral sections compared to the frontal ones.

Descriptive statistics – The middle section

For the middle axial sections, the following have been observed:

- lower CNR values for the maxillary jaw compared to the mandible,
- also lower CNR values in the lateral area compared to the frontal area,
- there are no major differences between regions, with the maxillary lateral area having the lowest CNR,
- the highest SD values were observed in the maxillary frontal area, so a higher image noise,
- the SD values in the maxillary sections compared to the mandibular ones were higher,
- the SD values of the frontal region were higher than the lateral one.

Descriptive statistics – The apical section

Regarding the apical axial sections, as central tendencies of the descriptive statistics, I found:

- lower CNR values for the maxillary jaw compared to the mandible,
- lower CNR values measured in the lateral area compared to the frontal area,
- in the maxillary lateral area, the CNR values were lower than in the other areas, so a poorer image quality,
- the lowest SD values were observed in the maxillary frontal area, so a lower image noise,
- the SD values in the maxillary sections compared to the mandibular ones were lower,
- SD values of the frontal region were decreased compared to the lateral region.

Descriptive statistics - The vicinity of other implants

From a descriptive point of view, depending on the proximity of the implants, I concluded the following:

- there are no significant differences in SD values between images with isolated implants or adjacent to other implants,
- CNR values of images with implants isolated or adjacent to other implants do not show significant differences.

Descriptive statistics - Position within the field of view

There are no descriptive significant differences in standard deviation (SD) and contrast-to-noise ratio (CNR) values between centrally or eccentrically placed field-of-view (FOV) implants.

Analytical statistics - Contrast-to-noise ratio

Comparison of mandibular and maxillary metal artifacts using the Mann-Whitney test showed that there was no significant difference in the number of artifacts, $P > 0.05$ (table VII.13.). When evaluating the artifacts of implants inserted in the anterior and posterior regions, the implants in the frontal region showed significantly more artifacts in all images, $P < 0.05$ (table VII.14.). Implants placed alone or in the vicinity of other implants (table VII.15.) did not show a significant difference in comparison ($P > 0.05$), nor did the evaluation of implants located centrally or eccentrically within the FOV (Table VII.16.).

Table VII.13. Comparison of mandibular and maxillary metal artefacts by CNR evaluation, according to the Mann-Whitney test

Secțiunea		Mediana	p
Cervical	maxilar	0.675	0.08
	mandibular	0.531	
Mediu	maxilar	0.661	0.12
	mandibular	0.709	
Apical	maxilar	0.622	0.22
	mandibular	0.696	

Table VII.14. Comparison of metal artifacts in the front and side areas by CNR evaluation, according to the Mann-Whitney test

Secțiunea		Mediana	p
Cervical	frontal	0.681	0.009*
	lateral	0.525	
Mediu	frontal	0.739	0.01*
	lateral	0.665	
Apical	frontal	0.825	<0.0001*
	lateral	0.538	

Table VII.15. Comparison of metal implants of implants according to the proximity of other implants by CNR evaluation, according to the Mann-Whitney test

Secțiunea		Mediana	p
Cervical	izolat	0.663	0.13
	adiacent	0.554	
Mediu	izolat	0.726	0.07
	adiacent	0.661	
Apical	izolat	0.724	0.13
	adiacent	0.662	

Table VII.16. Comparison of metal implants of implants according to position within FOV by CNR evaluation, according to the Mann-Whitney test

Secțiunea		Mediana	p
Cervical	central	0.639	0.25
	excentric	0.592	
Mediu	central	0.690	1
	excentric	0.670	
Apical	central	0.692	0.48
	excentric	0.672	

Kruskal-Wallis and Tukey tests revealed a statistically significantly greater difference in artifacts observed in cervical images compared to apical or middle images (Table VII.17.).

Table VII.17. Comparison of metal artifacts between cervical, middle and apical sections, by CNR evaluation

Secțiuni comparate		H	P
Cervical - Mediu	maxilar	4.85	0.18
	mandibular	23.12	<0.0001*
	frontal	1.27	0.73
	lateral	15.76	0.0012*
	izolat	13.28	0.06
	adiacent	15.59	0.02*
	centru FOV	20.3	0.0049*
	excentric FOV	17.51	0.01*
Cervical - Apical	maxilar	30.18	<0.0001*
	mandibular	21.62	<0.0001*
	frontal	9.31	0.025*
	lateral	19.27	0.00024*
	izolat	24	<0.0001*
	adiacent	29.32	0.00012*
	centru FOV	34.179	<0.0001*
	excentric FOV	22.62	0.0019*
Apical - Mediu	maxilar	39.08	<0.0001*
	mandibular	5.07	0.11
	frontal	6.46	0.09
	lateral	13.84	0.003*
	izolat	21.83	0.002*
	adiacent	52.341	<0.0001*
	centru FOV	28.16	0.0002*
	excentric FOV	21.27	0.0033*

Analytical statistics - Standard deviation

Comparison of mandibular and maxillary metal artifacts using the Mann-Whitney test showed that there was no significant difference in the number of artifacts, $P > 0.05$ (Table VII.18.), Nor in the assessment of the number of implant artifacts inserted in the

anterior regions. and posterior (tab. VII.19.), placed alone or in the vicinity of other implants (tab. VII.20.) or located centrally or eccentrically within the FOV (tab. VII.21.).

Table VII.18. Comparison of mandibular and maxillary metal artifacts by SD evaluation, according to the Mann-Whitney test

Secțiunea		Mediana	p
Cervical	maxilar	44.222	0.16
	mandibular	40.0745	
Mediu	maxilar	40.207	0.48
	mandibular	39.835	
Apical	maxilar	26.8555	0.07
	mandibular	30.833	

Table VII.19. Comparison of metal artifacts in the frontal and lateral areas by SD evaluation, according to the Mann-Whitney test

Secțiunea		Mediana	p
Cervical	frontal	42.9175	>0.05
	lateral	41.5715	
Mediu	frontal	40.644	0.22
	lateral	39.304	
Apical	frontal	27.153	0.59
	lateral	31.0065	

Table VII.20. Comparison of metal implants of implants in the vicinity of other implants by SD evaluation, according to the Mann-Whitney test

Secțiunea		Mediana	p
Cervical	izolat	43.331	0.67
	adiacent	42.161	
Mediu	izolat	41.477	0.63
	adiacent	39.782	
Apical	izolat	27.067	0.5
	adiacent	30.08	

Tabelul VII.21. Compararea artefactelor metalice ale implanturilor funcție de poziția în cadrul FOV prin evaluarea SD, conform testului Mann-Whitney

Secțiunea		Mediana	p
Cervical	central	42.8	0.5
	excentric	42.576	
Mediu	central	40.207	0.39
	excentric	39.835	
Apical	central	29.799	0.86
	excentric	27.361	

Kruskal-Wallis and Tukey tests revealed a statistically significantly greater difference in artifacts observed in cervical and middle images compared to apical images, $P < 0.05$, with higher SD values in cervical images (table VII.22.). When comparing the cervical and middle sections, although the differences between the groups were not large,

higher values were observed for the maxillary cervical sections ($P = 0.01$), the sections with adjacent implants and placed centrally in the FOV.

Table VII.22. Comparison of metal artifacts between cervical, middle and apical sections, by evaluating SD

Secțiuni comparate	H	P
Cervical-Mediu maxilar	10.2	0.01*
mandibular	0.43	0.93
frontal	6.77	0.07
lateral	3.66	0.3
izolat	3.79	0.8
adiacent	70.21	<0.0001*
centru FOV	19.73	0.006*
excentric FOV	9.31	0.23
Cervical-Apical maxilar	43.19	<0.0001*
mandibular	25.37	<0.0001*
frontal	43.99	<0.0001*
lateral	28.6	<0.0001*
izolat	28.37	0.0001*
adiacent	48.14	<0.0001*
centru FOV	44.56	<0.0001*
excentric FOV	29.12	<0.0001*
Apical-Mediu maxilar	36.92	<0.0001*
mandibular	21.33	<0.0001*
frontal	38.33	<0.0001*
lateral	20.59	0.0001*
izolat	23.23	0.0001*
adiacent	39.16	<0.0001*
centru FOV	40.19	<0.0001*
excentric FOV	23.58	0.0001*

7.5. Discussions

Early detection of bone changes around the implant can prevent redundant treatment, unnecessarily extended, and can reduce the risk of complications related to implant loss. So optimal image quality in CBCT is one of the desired properties. Highly absorbent materials, such as metal, act as a filter positioned inside the object, generating beam hardening artifacts

in direct relation with its density. If the X-ray beam is hardened, a nonlinear error will be recorded in the path of the beam behind the high-absorption materials, and this will be induced in the recorded data (Schulze *et al.*, 2011). In 3D reconstruction, the error is projected back in volume, resulting in either light streaks radiating from metal objects, or blackening of adjacent areas or even complete loss of gray values, reducing the contrast-to-noise ratio by decreasing the contrast and reducing the clarity of the areas of interest investigated. (Demirturk Kocasarac *et al.*, 2016; Katkar *et al.*, 2016).

In general, lesion-to-background contrast is related to the contrast-to-noise ratio, which is one of the main factors influencing image quality in CBCT. SD values allow a general estimate of darkness and brightness caused by high density materials, measured by varying gray values. So, a higher SD value or a higher variation indicates a higher artifact output. The magnitude of the artifacts was assessed by comparing the values obtained between the different regions examined, similar to previous research (Chindasombatjareon *et al.*, 2011; Bechara *et al.*, 2012a; Bechara *et al.*, 2012c; Oliveira *et al.*, 2013; Pauwels *et al.*, 2013; Benic *et al.*, 2013; Vasconcelos *et al.*, 2017; Kursun-Cakmak *et al.*, 2019). The protocol used in this research was selected according to the manufacturer's recommendations as the optimal exposure setting for an average adult patient, although it is known that exposure parameters should ideally take into account both patient characteristics and related specific diagnostic tasks indications to achieve dose reduction to satisfactory image quality (Nogah *et al.*, 1994; Katsumata *et al.*, 2006; Nakae *et al.*, 2008; Pauwels *et al.*, 2013; Bushberg, 2015; Panjnoush *et al.*, 2016; Oenning *et al.*, 2018).

In my study, according to the CNR evaluation, implants in the frontal region showed significantly more artifacts in all images, similar to previous studies, but when comparing mandibular and maxillary metal artifacts no significant difference was found in the number of artifacts, possibly due to the insufficient data number analyzed or the use of a small FOV of 4X4, so that the effect of exomass, ie the entire craniofacial area located inside and outside the FOV, more or less affected the measurements of gray value in the jaw and mandible (Benic *et al.* , 2013). In Machado's (2018) study, the number of artifacts was higher in the mandible and in the anterior regions, showing that the gray values of the object vary depending on its location and adjacent anatomical structures. Variations in the density and thickness of maxillary and mandibular bone tissue may explain the difference in the number of artifacts, which is consistent with the findings of Oliveira (2013), who evaluated the effect of anatomical localization on gray values in CBCT images and showed that the same object can have different values depending on the anatomical location. Comparison of SD values did not show any statistical difference between maxillary and mandibular or frontal and lateral regions, but all section images were affected by noise.

Artifacts, scatter radiation and noise in CBCT systems are not evenly spread across FOVs (Oliveira *et al.*, 2013). The current study was conducted to assess the effect of implant position in the visual field of view on CNR. According to the study of Valizadeh (2015), depending on the location in FOV, the sensitivity of the central position was significantly higher than that of the other positions, and the specificity was significantly higher at the position of 3 o'clock. Queiroz (2017), which evaluates the effect of an metal artifacts reduction instrument when the generating object was placed in different positions within the FOV, also noticed that the noise levels were different depending on the changes of position.

According to my study, centrally or eccentrically positioned implants in FOV did not make a significant difference when comparing CNR or SD.

In this study, when evaluating CNR, a higher number of artifacts was observed in the cervical third of the dental implant, similar to Machado's study (2018), probably only due to the presence of prosthetic crown, through its structure, intensifying the hardening of X radiation, whereas when comparing the number of artefacts around isolated implants with those around adjacent implants, no significant difference was observed in either cervical, middle or apical positions. From this point of view, future studies of comparative evaluation of artifacts in images with non-prosthetic implants are needed. One possible explanation is related to the use of a small ROI, so that the effect of adjacent implants was minimized in the middle and apical thirds. Prosthetic crown seems to be the one that generates the impressive decrease of CNR in the cervical area, its constituent metals being chromium (24), cobalt (27) or zirconia (40) alloys, which have higher atomic number than titanium (22) from the structure of the implants in the images analyzed in this study, generating an X-ray absorption and a larger beam hardening (Pauwels *et al.*, 2013; Kuusisto *et al.*, 2015). In the SD assessment, values were increased in the cervical and middle sections compared to the apical ones, possibly due to variations in bone density and thickness and greater distance from the roots of neighboring teeth and adjacent implants or the use of a small FOV of 4X4 mm and a small ROI, so that the effect of the exomass affected the measurements of the gray value less.

This study has some limitations. The first limitation is related to the small sample, then the use of a single data acquisition protocol, selected according to the manufacturer's recommendations as the optimal exposure setting for an average adult patient. Further research is needed with the use of the different types of scanners available on the market, assessing the influence of the various settings recommended by those manufacturers. It is essential to develop research that combines the number of artifacts with diagnostic accuracy until the actual level of interference of these unwanted images with clinical dental practice is found, as the need to improve resolution, including CNR, must be assessed in relation to radiation.

7.6. Conclusions

Early detection of bone changes around the implant can prevent redundant, unnecessarily extended treatments and can reduce the risk of complications from implant loss. Comparison of mandibular and maxillary metal artifacts using the Mann-Whitney test showed that there was no significant difference in the number of artifacts. When evaluating the number of implants related to the implants inserted in the anterior and posterior regions, the implants in the frontal region showed significantly more artifacts in all images. Implants placed alone or in the vicinity of other implants did not make a significant difference in comparison, nor did the evaluation of implants located centrally or peripherally in the FOV. Artifacts were observed predominantly in the cervical third of the dental implant, compared to the middle and apical thirds, most likely due to the presence of prosthetic crown.

GENERAL CONCLUSIONS

In everyday dental practice, CBCT imaging has become one of the essential ways of diagnosis. Consequently, for the efficient use of this technology, it is necessary to know its advantages and disadvantages, as well as its limitations. Artifacts generated by metal structures, through the effects of beam hardening and scatter radiation, affect the image quality to varying degrees, the main objective of artifacts investigation being to learn to reduce them if we fail to avoid them.

The presence of metal artifacts in CBCT images makes it necessary to evaluate methods that may reduce their occurrence in order to obtain reliable diagnostic information, so that personalized patient exposure and examination protocols can be developed in accordance with the ALARA principle (As Low As Reasonable Achievable).

As I have stated since the first study of this scientific research, the results obtained are difficult to interpret in terms of image quality, as there is no frame of reference for the parameters associated with metal artifacts.

In my doctoral research I quantitatively evaluated the effect of the metal presence in CBCT scans and correlated with the model and intensity of artifacts produced in order to identify the magnitude of these artifacts and the appropriate protocol for assessing a specific region in the vicinity of metal structures.

Personal scientific research has highlighted several important conclusions:

- the metal structures inserted at the level of the dental arches cause artifacts in all areas of the oral cavity, either by beam hardening or by scatter artifacts.

- the presence of metal structures at the level of the dental arches reduces the quality of CBCT images by increasing the image noise.

- the largest effect on the intensity of metal artifacts was the type of metal, the artifacts induced by cobalt-chromium alloy being more severe than those induced by titanium, the images resulting from the scans of chromium-cobalt alloy being more affected by different protocols than titanium.

- artifacts due to the beam-hardening effect are predominantly observed in the case of titanium scans. In the case of chromium-cobalt alloy scans compared to those of titanium, scattering artifacts appear in the evaluated vestibular and oral areas, and the present beam-hardening effects are lower compared to titanium.

- the artefacts were more intense in the anterior vestibular area in the case of titanium and in the posterior lingual / molar area in the case of the Cr-Co alloy, the evaluation of the image in these areas being necessary to be done with caution.

- the variation of the tube current did not affect the metal artifacts, and the increase in voltage caused the reduction of the artifacts in the positions adjacent lingual and vestibular to the canine and molar areas, but did not reduce the artifacts in the intermediate positions between canine and premolar or premolar and molar, although the CBCT scanner used did not allow the absolute effect of kVp and mA to be studied in a relevant range.

- the exposure protocols used acted differently for each of the metal structures inserted, both in terms of material and position, the choice of acquisition protocol being able to influence the image quality required for diagnosis and radiation dose for the patient.

- there is no general exposure protocol suitable for the assessment of the entire oral cavity, but there are settings configurations of the exposure parameters according to different diagnostic tasks that would help to make professional decisions about the protocol of choice for specific clinical indications, which must be correlated with the ALARA principle. In this context, future studies are encouraged to establish exposure protocols that promote a good relationship between exposure dose and CBCT image quality in assessing the regions around implants.

- the measurement of metal artifacts in CBCT devices shows a wide range of values, determined by the variety of imaging parameters used in the study. For this reason, in clinical practice, the diagnosis of the area between adjacent metal objects should be avoided, as these regions show an excessive loss of projection information, due to the effects of beam strengthening, with the risk of false positive diagnoses. For other affected regions in the vicinity of the metal, the assessment of the image should be done with caution, and in particular avoid quantitative measurements based on voxel values, the degradation of the image quality being obvious.

- The intensity of the artifacts produced in CBCT images was high in the regions close to the metallic structures, but it is necessary to evaluate the interference of the artifacts in the diagnosis of pathological conditions adjacent to these structures, so the link between subjective and objective image quality.

- we found a larger number of artifacts in the mandible and in the anterior regions, with variations depending on the location of the implant and the adjacent anatomical structures in terms of varying density and thickness of bone tissue, but the position of the implants in the field of view did not make a significant difference. in comparison, also their proximity.

- the evaluated artifacts were observed predominantly in the cervical third of the dental implant, probably due to the presence of prosthetic work, when evaluating the gray values being small differences in favor of sections with adjacent implants and placed centrally in FOV.

- the metal artifact assessment method used, based on the differences in the gray tones of the pixels of the two-dimensional CBCT images of the metal structures, can provide a good quantitative assessment of the artifacts from the perspective of dental materials. Therefore, I believe that this method is more reliable compared to eye identification.

- knowledge of the differences between artifacts, caused by various metallic materials, their location and exposure protocols, could facilitate clinical decisions for the choice of material or imaging device settings.

One of the most relevant conclusions based on the results obtained in my doctoral research is that the possibility of reducing metal artifacts based on the adjustment of exposure parameters is very limited. Although some reduction in the artifacts can be seen when comparing the different exposure protocols of the same device used in this research, the effect on the artifacts is quite small and no increase in radiation dose can be justified for the sole purpose of reducing the artifacts.

Also, in the summary of the presented, the CBCT user has limited possibilities to reduce the artifacts. Therefore, researchers and manufacturers need to combine their efforts in optimizing exposure factors and implementing metal artifact reduction algorithms.

The results obtained must be seen from the perspective of **limitations**, in the case of the first study they are determined by the use of a uniform model in laboratory conditions, which makes the impact of anthropomorphic phantom models theoretical, so the comparison was based on basic knowledge of medical physics. and X-ray attenuation characteristics. Other limitations of the first study were the comparison of only two types of metal with the use of a single CBCT unit model with its characteristic exposure parameters.

In the second study, the limitations are related to a relatively small number of cases, only prosthetic implants, and last but not least, a single exposure protocol of the same CBCT equipment, a protocol that was selected according to the manufacturer's recommendations as the optimal exposure setting for an average adult patient, so I did not evaluate the influence of the various settings recommended by other manufacturers.

It is also worth mentioning the need for further evaluation of exposure protocols in relation to the radiation dose to the patient and the relationship between objective, measured quality, and subjective image quality, which must include both psycho-physical and environmental considerations. system to predict therapeutic impact.

All this adds to the context in which my doctoral research focused only on a section of the approached field, that of CBCT technology, which is in a dynamic development, proposing in the future to **continue the research** in the aforementioned directions.

From this perspective, further studies should be conducted on the production of artifacts by other high-density materials, such as zirconia implants, orthodontic brackets, and prosthetic crowns, to look for protocols that provide effective reductions in image artifact expression.

At the same time, as we observed different behavior between different protocols, regions and types of metals, new studies should be conducted to assess the extent of artifacts produced by various metal restorative materials in various CBCT units, which differ in several features, such as would be image receiver technology and mathematical algorithms for image reconstruction, which can also influence image formation and artifact expression.

Given the widespread use of CBCT and the importance of artifacts in clinical dentistry, and the variability of outcomes, all practitioners should be aware of how artifacts are expanded in their own scanners if working with units other than those used in this research.

Given that the methodology used in this thesis for the evaluation of metal artifacts is time consuming, requires knowledge in several fields, my intention is to continue research on this topic so as to identify a more accurate and reliable method of evaluating artifacts, more suitable for dental CBCT characteristics and more convenient for on-site operation in radiodiagnostic clinics.

My doctoral research brings **new elements** to the current state of knowledge in the field, by clarifying some aspects of optimization for CBCT exams, currently existing guides being a means of standardizing and improving image quality, but with a gap between evidence and practice, studies from the literature presenting heterogeneous, sometimes

contradictory conclusions and working methodologies, so that the comparative analysis must be viewed with caution.

The studies presented in this thesis covered a number of different aspects of the use of CBCT in dentistry, their original character resulting from the topic addressed, characteristic of a niche segment in the field of CBCT imaging, that of metal artifacts, and also in terms of results. obtained, the evaluation being performed by addressing several variables. The results of my studies are related to the magnitude of the metal artifacts that affect the images, a situation frequently encountered in current practice and which every practitioner must take into account when diagnosing and developing the treatment plan.

The authenticity of the paper also results from the experimental use of settings configurations of exposure parameters depending on the investigated area correlated with the type of metal present, in accordance with different diagnostic tasks, which can help to achieve customized exposure protocols. In addition, by recognizing the magnitude of metal artifacts present in CBCT images of implants based on their number and the anatomical region where they are inserted, my research contributes to the early detection of bone changes around the implant, which can prevent redundant treatments and investigations.

SELECTIVE BIBLIOGRAPHY

Barrett, J. F., & Keat, N. (2004). Artifacts in CT: recognition and avoidance. *Radiographics* : a review publication of the Radiological Society of North America, Inc, 24(6), 1679–1691. <https://doi.org/10.1148/rg.246045065>

Bechara, B., McMahan, C. A., Geha, H., & Noujeim, M. (2012a). Evaluation of a cone beam CT artefact reduction algorithm. *Dento maxillo facial radiology*, 41(5), 422–428. <https://doi.org/10.1259/dmfr/43691321>

Bechara, B. B., Moore, W. S., McMahan, C. A., & Noujeim, M. (2012b). Metal artefact reduction with cone beam CT: an in vitro study. *Dento maxillo facial radiology*, 41(3), 248–253. <https://doi.org/10.1259/dmfr/80899839>

Bechara, B., McMahan, C. A., Moore, W. S., Noujeim, M., Geha, H., & Teixeira, F. B. (2012c). Contrast-to-noise ratio difference in small field of view cone beam computed tomography machines. *Journal of oral science*, 54(3), 227–232. <https://doi.org/10.2334/josnusd.54.227>

Benic, G. I., Sancho-Puchades, M., Jung, R. E., Deyhle, H., & Hämmerle, C. H. (2013). In vitro assessment of artifacts induced by titanium dental implants in cone beam computed tomography. *Clinical oral implants research*, 24(4), 378–383. <https://doi.org/10.1111/clr.12048>

Bushberg, J.T. (2015). Eleventh annual Warren K. Sinclair keynote address-science, radiation protection and NCRP: building on the past, looking to the future. *Health physics*, 108 2, 115-23 .

Chindasombatjareon J, Kakimoto N, Murakami S, Maeda Y, Furukawa S. (2011) Quantitative analysis of metallic artifacts caused by dental metals: comparison of cone-beam and multi-detector row CT scanners. *Oral Radiol.* Dec;27(2):114-20. <https://doi.org/10.1016/j.fdj.2016.04.001>

de Man B. (1999) Metal streak artefacts in X-ray computed tomography: a simulation study. *IEEE Trans Nuc Sci*; 46:691–696 <https://doi.org/10.1109/23.775600>

de Man B. (2000) Reduction of metal streak artefacts in X-ray computed tomography using a transmission maximum a posteriori algorithm. *IEEE Trans Nuclear Sci*; 47:977–981 <https://doi.org/10.1109/23.856534>

Demirturk Kocasarac, H., Helvacioğlu Yigit, D., Bechara, B., Sinanoglu, A., & Noujeim, M. (2016). Contrast-to-noise ratio with different settings in a CBCT machine in presence of different root-end filling materials: an in vitro study. *Dento maxillo facial radiology*, 45(5), 20160012. <https://doi.org/10.1259/dmfr.20160012>

Directiva 96/29/Euratom a Consiliului Uniunii Europene, 1996. <http://data.europa.eu/eli/dir/1996/29/oj>

Draenert, F. G., Copenrath, E., Herzog, P., Müller, S., & Mueller-Lisse, U. G. (2007). Beam hardening artefacts occur in dental implant scans with the NewTom cone beam CT but not with the dental 4-row multidetector CT. *Dento maxillo facial radiology*, 36(4), 198–203. <https://doi.org/10.1259/dmfr/32579161>

Fontenele, R. C., Nascimento, E. H., Vasconcelos, T. V., Noujeim, M., & Freitas, D. Q. (2018). Magnitude of cone beam CT image artifacts related to zirconium and titanium implants: impact on image quality. *Dento maxillo facial radiology*, 47(6), 20180021. <https://doi.org/10.1259/dmfr.20180021>

Holberg, C., Steinhäuser, S., Geis, P., & Rudzki-Janson, I. (2005). Cone-beam computed tomography in orthodontics: benefits and limitations. *Journal of orofacial orthopedics = Fortschritte der Kieferorthopädie : Organ/official journal Deutsche Gesellschaft für Kieferorthopädie*, 66(6), 434–444. <https://doi.org/10.1007/s00056-005-0519-z>

Hunter, A., McDavid, D. (2009). Analyzing the beam hardening artifact in the Planmeca Promax. *Oral Surg Oral Med Oral Pathol Oral Radiol Endod.*, 107(4): e28-9.

[Jones, A. A., & Cochran, D. L. \(2006\). Consequences of implant design. *Dental clinics of North America*, 50\(3\), 339–v. https://doi.org/10.1016/j.cden.2006.03.008](https://doi.org/10.1016/j.cden.2006.03.008)

Kamburoğlu, K., Gülşahi, A., Genç, Y., & Paksoy, C. S. (2012). A comparison of peripheral marginal bone loss at dental implants measured with conventional intraoral film

and digitized radiographs. *The Journal of oral implantology*, 38(3), 211–219.
<https://doi.org/10.1563/AAID-JOI-D-09-00147>

Katkar, R., Steffy, D. D., Noujeim, M., Deahl, S. T., 2nd, & Geha, H. (2016). The effect of milliamperage, number of basis images, and export slice thickness on contrast-to-noise ratio and detection of mandibular canal on cone beam computed tomography scans: an in vitro study. *Oral surgery, oral medicine, oral pathology and oral radiology*, 122(5), 646–653. <https://doi.org/10.1016/j.oooo.2016.08.006>

[King, G. N., Hermann, J. S., Schoolfield, J. D., Buser, D., & Cochran, D. L. \(2002\). Influence of the size of the microgap on crestal bone levels in non-submerged dental implants: a radiographic study in the canine mandible. *Journal of periodontology*, 73\(10\), 1111–1117. <https://doi.org/10.1902/jop.2002.73.10.1111>](https://doi.org/10.1016/j.oooo.2016.08.006)

Kursun-Cakmak, E. Ş., Demirturk Kocasarac, H., Bayrak, S., Ustaoglu, G., & Noujeim, M. (2019). Estimation of contrast-to-noise ratio in CT and CBCT images with varying scan settings in presence of different implant materials. *Dento maxillo facial radiology*, 48(8), 20190139. <https://doi.org/10.1259/dmfr.20190139>

Kuusisto, N., Vallittu, P. K., Lassila, L. V., & Huuonen, S. (2015). Evaluation of intensity of artefacts in CBCT by radio-opacity of composite simulation models of implants in vitro. *Dento maxillo facial radiology*, 44(2), 20140157. <https://doi.org/10.1259/dmfr.20140157>

Kyriakou, Y., Prell, D., & Kalender, W. A. (2009). Ring artifact correction for high-resolution micro CT. *Physics in medicine and biology*, 54(17), N385–N391. <https://doi.org/10.1088/0031-9155/54/17/N02>

Loubele, M., Bogaerts, R., Van Dijck, E., Pauwels, R., Vanheusden, S., Suetens, P., Marchal, G., Sanderink, G., & Jacobs, R. (2009). Comparison between effective radiation dose of CBCT and MSCT scanners for dentomaxillofacial applications. *European journal of radiology*, 71(3), 461–468. <https://doi.org/10.1016/j.ejrad.2008.06.002>

Machado, A. H., Fardim, K., de Souza, C. F., Sotto-Maior, B. S., Assis, N., & Devito, K. L. (2018). Effect of anatomical region on the formation of metal artefacts produced by dental implants in cone beam computed tomographic images. *Dento maxillo facial radiology*, 47(3), 20170281. <https://doi.org/10.1259/dmfr.20170281>

Nakae, Y., Sakamoto, K., Minamoto, T., Kamakura, T., Ogata, Y., Matsumoto, M., & Johkou, T. (2008). Clinical evaluation of a newly developed method for avoiding artifacts caused by dental fillings on X-ray CT. *Radiological physics and technology*, 1(1), 115–122. <https://doi.org/10.1007/s12194-007-0016-8>

Oliveira, M. L., Tosoni, G. M., Lindsey, D. H., Mendoza, K., Tetradis, S., & Mallya, S. M. (2013). Influence of anatomical location on CT numbers in cone beam computed tomography. *Oral surgery, oral medicine, oral pathology and oral radiology*, 115(4), 558–564. <https://doi.org/10.1016/j.oooo.2013.01.021>

Panjnoush, M., Kheirandish, Y., Kashani, P. M., Fakhar, H. B., Younesi, F., & Mallahi, M. (2016). Effect of Exposure Parameters on Metal Artifacts in Cone Beam Computed Tomography. *Journal of dentistry (Tehran, Iran)*, 13(3), 143–150.

Parsa, A., Ibrahim, N., Hassan, B., Syriopoulos, K., & van der Stelt, P. (2014). Assessment of metal artefact reduction around dental titanium implants in cone beam CT. *Dento maxillo facial radiology*, 43(7), 20140019. <https://doi.org/10.1259/dmfr.20140019>

Pauwels, R., Araki, K., Siewerdsen, J. H., & Thongvigitmanee, S. S. (2015). Technical aspects of dental CBCT: state of the art. *Dento maxillo facial radiology*, 44(1), 20140224. <https://doi.org/10.1259/dmfr.20140224>

Perrella, A., Lopes, P. M., Rocha, R. G., Fenyó-Pereira, M., & Cavalcanti, M. G. (2010). Influence of dental metallic artifact from multislice CT in the assessment of simulated mandibular lesions. *Journal of applied oral science : revista FOB*, 18(2), 149–154. <https://doi.org/10.1590/s1678-77572010000200009>

Prell, D., Kyriakou, Y., Beister, M., & Kalender, W. A. (2009). A novel forward projection-based metal artifact reduction method for flat-detector computed tomography. *Physics in medicine and biology*, 54(21), 6575–6591. <https://doi.org/10.1088/0031-9155/54/21/009>

Queiroz, P. M., Santaella, G. M., da Paz, T. D., & Freitas, D. Q. (2017). Evaluation of a metal artefact reduction tool on different positions of a metal object in the FOV. *Dento maxillo facial radiology*, 46(3), 20160366. <https://doi.org/10.1259/dmfr.20160366>

Razavi, T., Palmer, R. M., Davies, J., Wilson, R., & Palmer, P. J. (2010). Accuracy of measuring the cortical bone thickness adjacent to dental implants using cone beam computed tomography. *Clinical oral implants research*, 21(7), 718–725. <https://doi.org/10.1111/j.1600-0501.2009.01905.x>

Scarfe, W. C., & Farman, A. G. (2008). What is cone-beam CT and how does it work?. *Dental clinics of North America*, 52(4), 707–v. <https://doi.org/10.1016/j.cden.2008.05.005>

Schulze, R. K., Berndt, D., & d'Hoedt, B. (2010). On cone-beam computed tomography artifacts induced by titanium implants. *Clinical oral implants research*, 21(1), 100–107. <https://doi.org/10.1111/j.1600-0501.2009.01817.x>

Schulze, R., Heil, U., Gross, D., Bruellmann, D. D., Dranischnikow, E., Schwanecke, U., & Schoemer, E. (2011). Artefacts in CBCT: a review. *Dento maxillo facial radiology*, 40(5), 265–273. <https://doi.org/10.1259/dmfr/30642039>

SEDEXCT Project. European Commission, Directorate-General for Energy, (2012). Cone beam CT for dental and maxillofacial radiology : evidence-based guidelines, Publications Office. <https://data.europa.eu/doi/10.2768/21874>

Suomalainen, A. K., Salo, A., Robinson, S., & Peltola, J. S. (2007). The 3DX multi image micro-CT device in clinical dental practice. *Dento maxillo facial radiology*, 36(2), 80–85. <https://doi.org/10.1259/dmfr/30358216>

Tyndall, D. A., Price, J. B., Tetradis, S., Ganz, S. D., Hildebolt, C., Scarfe, W. C., & American Academy of Oral and Maxillofacial Radiology (2012). Position statement of the American Academy of Oral and Maxillofacial Radiology on selection criteria for the use of radiology in dental implantology with emphasis on cone beam computed tomography. *Oral surgery, oral medicine, oral pathology and oral radiology*, 113(6), 817–826. <https://doi.org/10.1016/j.oooo.2012.03.005>

Vasconcelos, T. V., Bechara, B. B., McMahan, C. A., Freitas, D. Q., & Noujeim, M. (2017). Evaluation of artifacts generated by zirconium implants in cone-beam computed tomography images. *Oral surgery, oral medicine, oral pathology and oral radiology*, 123(2), 265–272. <https://doi.org/10.1016/j.oooo.2016.10.021>

Valizadeh, S., Vasegh, Z., Rezapanah, S., Safi, Y., & Khaezifard, M. J. (2015). Effect of Object Position in Cone Beam Computed Tomography Field of View for Detection of Root Fractures in Teeth with Intra-Canal Posts. *Iranian journal of radiology : a quarterly journal published by the Iranian Radiological Society*, 12(4), e25272. <https://doi.org/10.5812/iranradiol.25272>

Wang, Q., Li, L., Zhang, L., Chen, Z., & Kang, K. (2013). A novel metal artifact reducing method for cone-beam CT based on three approximately orthogonal projections. *Physics in medicine and biology*, 58(1), 1–17. <https://doi.org/10.1088/0031-9155/58/1/1>

White SC, Pharoah MJ. (2014) *Oral radiology: principles and interpretation*. 7th Ed., St. Louis, Missouri, Elsevier-Mosby. eText ISBN: 9780323096331